

## Dynamical Feedbacks and the Persistence of the NAO

ELIZABETH A. BARNES AND DENNIS L. HARTMANN

*Department of Atmospheric Sciences, University of Washington, Seattle, Washington*

(Manuscript received 4 May 2009, in final form 29 September 2009)

### ABSTRACT

The persistence of the North Atlantic Oscillation (NAO) is studied using observations of the three-dimensional vorticity budget in the Atlantic sector. Analysis of the relative vorticity tendency equation shows that convergence of eddy vorticity flux in the upper troposphere counteracts the effect of anomalous large-scale divergence at the upper level. At low levels, the convergence associated with this large-scale vertical circulation cell maintains the relative vorticity anomaly against frictional drag. The eddy vorticity flux convergence thus acts to sustain the vorticity anomaly associated with the NAO against drag and increases the persistence of the NAO vorticity anomaly. The adiabatic cooling associated with the rising motion in the vorticity maximum sustains the thermal structure of the NAO anomaly, enhancing the baroclinicity, and thus eddy generation. This constitutes a positive eddy feedback that helps maintain the NAO. The positive eddy feedback occurs only in the midlatitude region and is strongest during the negative phase of the NAO when the Atlantic jet is displaced toward the equator, with a high pressure anomaly to the north and a low pressure anomaly to the south. The stronger feedback demonstrated during the negative phase is consistent with the greater persistence observed for this phase of the NAO. The positive feedback appears to be associated with anomalous northward eddy propagation away from the jet.

### 1. Introduction

In 1924, Gilbert T. Walker coined the name “North Atlantic Oscillation” (NAO) for the well-known swaying of pressure anomalies between the Azores and Iceland (Walker 1924). Today, this teleconnection pattern is known to be a poleward (equatorward) shift of the Atlantic jet when the NAO is in its high (low) phase, affecting the weather over western Europe and Greenland (Vallis and Gerber 2008; Hurrell et al. 2003). While Feldstein (2000) found the *e*-folding time of the NAO to be approximately 10 days, Rennert and Wallace (2009) argue that it is not so much the *e*-folding time as the broad shoulder of the NAO’s autocorrelation at intermediate time scales (10–30 days) that distinguishes this teleconnection pattern from other modes of atmospheric variability. The results presented here provide a possible explanation for this extended persistence.

The distinction between the NAO and the hemispheric variability of the Northern Hemisphere extra-

tropical jet, coined the northern annular mode (NAM), has been a topic of debate (Thompson and Wallace 1998, 2000; Ambaum et al. 2001). In the zonal mean, the annular mode is the leading mode of variability in each hemisphere and manifests itself as a latitudinal shifting of the eddy-driven jet (Lorenz and Hartmann 2001, 2003; hereafter LH01 and LH03). LH03 demonstrated that the Northern Hemisphere jet remained in a shifted position for an extended period of time due to a positive eddy–zonal flow feedback. LH03 identified the synoptic eddies (high-pass 15-day filter) as the main contributors to this positive feedback, where the low-frequency flow organizes the high-frequency eddies in such a way as to extend the low-frequency anomaly persistence. They also demonstrated that the second leading mode of hemispheric variability is associated with a strengthening and sharpening of the jet; it exhibits a weak feedback and thus lacks the persistence of the NAM.

Building from the work of LH03, Eichelberger and Hartmann (2007) studied the leading mode of variability for zonally averaged flow in the Atlantic and Pacific sectors during Northern Hemisphere winter. They found that the leading mode of the Atlantic corresponds well with the NAM, while the leading mode of the Pacific is a combination of a latitudinal shifting and a pulsing of the

---

*Corresponding author address:* Elizabeth A. Barnes, Department of Atmospheric Sciences, University of Washington, Box 351640, Seattle, WA 98195.  
E-mail: eabarnes@atmos.washington.edu

jet. Eichelberger and Hartmann proposed that the amplitude of the annular mode over the Pacific sector is reduced owing to the weak eddy–zonal flow feedbacks associated with a stronger Hadley-driven subtropical jet. In this scenario, the feedbacks are weakened in the strong subtropical jet due to the stronger waveguide inhibiting the meridional propagation of the waves and ducting the waves downstream where they break when the jet ends. This can act to extend the jet but not to maintain meridional displacement.

Multiple studies have suggested that the positive feedback between the eddies and the low-frequency flow sustains the low-frequency anomalies against surface drag (Feldstein and Lee 1998; Robinson 2000; Gerber and Vallis 2007; Hartmann 2007). Robinson (1996, 2000) demonstrated the importance of surface drag to the eddy-feedback interaction responsible for the extended persistence of the zonal index. With a poleward shift of the jet, the eddy fluxes produce a poleward transport of heat, which typically reduces the baroclinicity in the region of the shifted jet (and thus restricts the production of more eddies). However, in the presence of drag, the poleward transport of heat, and thus destruction of the temperature gradient, is balanced by the adiabatic cooling from a thermally indirect Ferrel cell, which moves momentum supplied by eddy fluxes at upper levels to the surface (Hartmann and Lo 1998; Robinson 2006; Hartmann 2007).

The positive-feedback mechanisms described thus far have all been in a zonal-mean framework. Allowing for zonal asymmetries, Feldstein (2003) studied the dynamics of the NAO growth and decay by performing composite analysis on each term in the 300-mb streamfunction tendency equation during individual NAO life cycles (defined by a set of criteria). Using this composite life cycle technique, Feldstein showed that the high-frequency (10-day filtered) eddy forcing pattern projects positively onto the NAO pattern after the onset of the NAO, while the divergence term and low-frequency eddy forcing project negatively and thus contribute to the decay of the NAO. We find similar relationships. We further show that the eddy vorticity flux convergence at upper levels is important to sustaining the vorticity maximum against divergence. The divergence at upper levels can be thought of as part of the geostrophic adjustment to the vorticity convergence, and the vertical motion cools the column to maintain a vortex maximum in the presence of eddy heat convergences that would otherwise cause the vortex to weaken. The eddy vorticity flux convergences at upper levels thus contribute to maintaining both the momentum and temperature anomalies associated with a strong vorticity maximum.

The primary goal of this study is to demonstrate quantitatively that the net eddy flow of vorticity during the NAO constitutes a positive feedback that together with the implied vertical motion field extends the NAO's persistence. This goal is achieved by linking individual terms in the relative vorticity tendency equation with upper- and lower-level tropospheric processes in a time series analysis framework, which admits a quantitative description of the feedback strength. This analysis technique is also used to explore asymmetries in the positive feedback over different spatial locations of the Atlantic and during the two phases of the NAO.

## 2. Data

The data consists of 43 years (1959–2001) of  $2.5^\circ \times 2.5^\circ$  latitude–longitude gridded daily (1200 UTC) sea level pressure (SLP), zonal velocity  $u$ , meridional velocity  $v$ , and the vertical component of relative vorticity [ $\zeta = \nabla \times \mathbf{u}$  where  $\mathbf{u} = (u, v)$ ] on 13 vertical levels (1000, 925, 850, 775, 700, 600, 500, 400, 300, 250, 200, 150, and 100 mb) from the European Centre for the 40-yr Medium-Range Weather Forecasts Re-Analysis (ERA-40) (Uppala et al. 2005). Only Northern Hemisphere wintertime [December–March (DJFM)] fields are analyzed in this paper, and the time series analysis is applied to each 121-day winter season of DJFM (thus ignoring 29 February during leap years). To aid in visualization, we have filtered the plots of spatial fields by expanding in spherical harmonics and truncating at T27.

To analyze the variability of the atmosphere, we define daily anomaly data throughout this paper by removing the mean seasonal cycle. The mean seasonal cycle is a smooth curve computed as the annual mean plus the first four Fourier harmonics of the daily climatology for all seasons over the 43 years of data. Thus, the magnitude of a variable  $x$  at a single location can be decomposed into a climatological value  $\bar{x}$  plus an anomalous value  $\hat{x}$  such that  $x = \bar{x} + \hat{x}$ . Part of this analysis requires splitting the anomalous fields into high- and low-frequency components, representing variability on time scales less than and greater than 7 days, respectively. This frequency division used a 7-day cutoff Lanczos filter with 41 weights (Hamming 1989) applied to all seasons over the 43 years. The DJFM fields were retained after frequency filtering was performed on the entire dataset including all months.

## 3. Low-frequency variability in the Atlantic sector

The NAO pattern explains the largest amount of the variance of DJFM low-frequency sea level pressure variability over the Atlantic (Hurrell et al. 2003). Empirical

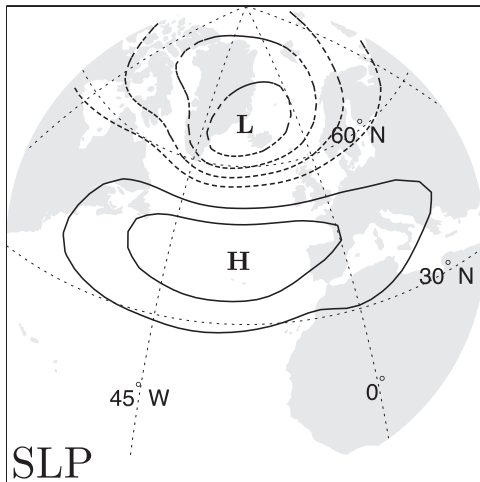


FIG. 1. Leading EOF of DJFM monthly-mean sea level pressure over the Atlantic region 25°–90°N, 90°W–30°E. Contours are drawn every 2.6 mb with negative contours dashed and zero contour line omitted.

orthogonal function (EOF) analysis of the monthly-mean sea level pressure anomalies in the Atlantic sector (25°–90°N, 90°W–30°E) results in a leading pattern (leading EOF) for which we define the high phase to be a low pressure center over Greenland and a high pressure center in the midlatitudes of the Atlantic Ocean, as shown in Fig. 1. The structure is displayed in units of millibars and not in normalized form and explains 38% of the month-to-month variance of winter sea level pressure in the Atlantic sector. Before performing EOF analysis, the data were properly weighted to account for the decrease in area toward the pole. The structure obtained is not sensitive to the exact Atlantic region used and is distinct from the other eigenvectors according to the criterion outlined by North et al. (1982).

The following results use an NAO index  $Z(t)$  defined by projecting daily sea level pressure anomalies onto the NAO structure previously defined. The time series  $Z(t)$  is normalized to have a standard deviation of one as is convention. Note that the NAO index has a mean of zero by construction. NAO patterns in fields other than sea level pressure are obtained by regressing  $Z(t)$  onto the daily anomaly maps.

The NAO describes a north–south oscillation of the eddy-driven jet, with the high phase defined as a poleward shift of the jet from its climatological position (anomalously low sea level pressure over Greenland as depicted in Fig. 1) and the low phase as an equatorward shift of the jet. This jet shift is also evident in the mass-weighted upper-level (300, 250, 200, 150 mb) relative vorticity field displayed in Fig. 2b. The high-phase NAO denotes an anomalous increase in cyclonic vorticity to

the north when compared to the winter-mean field shown in Fig. 2a, 90 degrees out of phase with the shift in upper-level zonal wind. The boxed regions in Figs. 2b,c define the “north lobe” (55°–70°N, 50°W–0°) and “south lobe” (37°–55°N, 50°W–0°), and both lobes together are termed the “NAO region” (37°–70°N, 50°W–0°). The conclusions of this paper are robust with respect to different regional definitions.

Figure 2c shows the mass-weighted NAO vorticity pattern at lower levels (1000, 925, 850 mb). At these levels, the lobe over Greenland (north lobe) is significantly smaller in area than the south lobe. Comparing to Fig. 2b, the centroid of the upper-level vorticity pattern lies to the west of the centroid of the lower-level structure, indicating a westward tilt with height.

#### 4. Vorticity budget

The relative vorticity tendency at a given horizontal location and vertical pressure level is given by (Holton 2004)

$$\frac{\partial \zeta}{\partial t} = -\nabla \cdot [(\zeta + f)\mathbf{u}] - \omega \frac{\partial \zeta}{\partial p} + \hat{\mathbf{k}} \cdot \left( \frac{\partial \mathbf{u}}{\partial p} \times \nabla \omega \right) + \mathcal{F}, \tag{1}$$

where  $\nabla \cdot$  and  $\nabla$  denote the 2D horizontal divergence and gradient respectively,  $f$  is the Coriolis parameter,  $\omega$  the vertical velocity; and  $\mathcal{F}$  the forcing due to friction. Using simple scaling arguments (as done in Holton 2004), one can show that the vertical advection of vorticity and the tilting term (second and third right-hand terms) in (1) are an order of magnitude smaller than the convergence of vorticity flux (first right-hand term). Splitting the relevant terms in (1) into seasonal-mean and anomalous quantities (see section 2 for details) and rearranging terms yields an equation for the anomalous vorticity tendency:

$$\begin{aligned} \frac{\partial \hat{\zeta}}{\partial t} = & [-(\bar{\zeta} + f)\mathbf{V} \cdot \hat{\mathbf{u}} - \hat{\zeta}\mathbf{V} \cdot \bar{\mathbf{u}}]_{\text{stretching}} + [-\mathbf{V} \cdot (\hat{\zeta}\hat{\mathbf{u}})]_{\text{eddy}} \\ & + [-\hat{\mathbf{u}} \cdot \nabla(\bar{\zeta} + f) - \bar{\mathbf{u}} \cdot \nabla \hat{\zeta}]_{\text{wave}} \\ & + \{-\mathbf{V} \cdot [\bar{\mathbf{u}}(\bar{\zeta} + f)]\}_{\text{clim}} + \mathcal{F}, \end{aligned} \tag{2}$$

where we have made the approximation that  $\partial \hat{\zeta} / \partial t \gg \partial \bar{\zeta} / \partial t$  (the climatological-mean vorticity tendency is not identically equal to zero due to its seasonal component).

The first term on the rhs of (2) is the vorticity source due to divergence, often referred to as the “stretching term.” Analysis of each quantity in the stretching term shows that the vorticity source due to the mean divergence has a negligible effect on the NAO vorticity

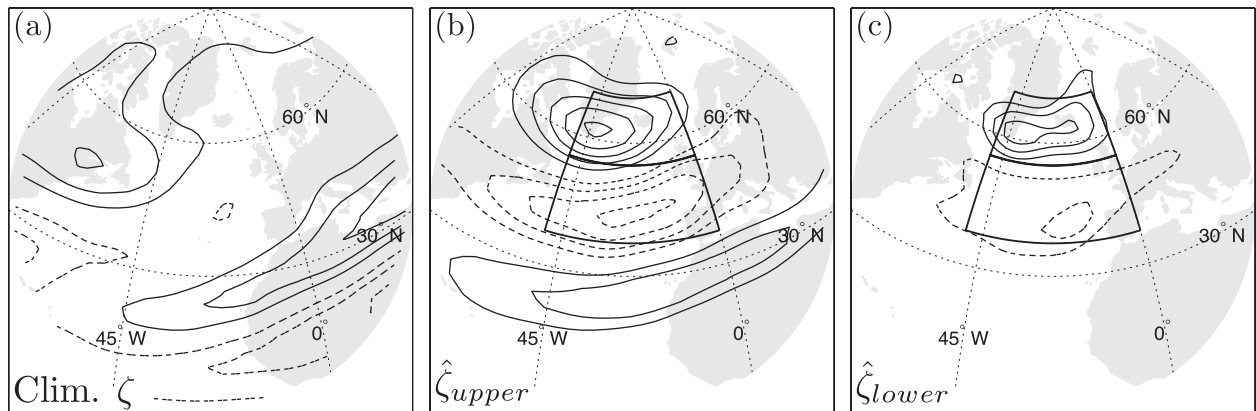


FIG. 2. (a) Mean climatological relative vorticity at 250 mb and NAO structures of relative vorticity for the mass-weighted (b) upper-level (300, 250, 200, 150 mb) and (c) lower-level (1000, 925, 850 mb) relative vorticity. Contours are drawn every  $9 \times 10^{-6} \text{ s}^{-1}$  for (a) and every  $3.5 \times 10^{-6} \text{ s}^{-1}$  for (b) and (c), negative contours dashed. The NAO region used for the feedback analysis is overlaid with the north and south lobe regions as the north and south sectors, respectively. The zero contour line has been omitted.

tendency, although it will be included in this analysis for completeness. The second rhs term represents the forcing of the anomalous vorticity by the divergence of the anomalous vorticity flux and will be termed the “eddy forcing.” The third term of (2) is the linear wave term, composed of the advection of the background vorticity by the anomalous wind and the advection of the anomalous vorticity by the mean wind. The fourth term is composed of seasonal-mean quantities and represents the climatological vorticity flux convergence (stationary wave forcing), which is nearly constant throughout the winter season.

## 5. Feedback mechanism

In this section, we present a feedback mechanism that compensates for the effect of surface drag and enables persistence and self-maintenance of the NAO pattern. It is important to note that this mechanism is similar to the mechanisms described by previous authors (Gerber and Vallis 2007; Hartmann 2007; Robinson 2000, 2006) in a zonal-mean framework. Figure 3 depicts the proposed mechanism for a region of anomalous positive vorticity, with the anomalous westerly zonal wind located equatorward of the vorticity anomaly. Since the midlatitude, upper-level jet is a source of eddies, we expect that a meridional jet shift will be accompanied by a shift in the baroclinic zone and, thus, a shift in the eddy source region (Hartmann 2007). In our vorticity framework, the eddies will propagate and break away from the source region, producing a convergence of eddy vorticity flux at upper levels and reinforcing the positive vorticity anomaly associated with the NAO. The convergence of eddy vorticity flux in the upper levels is balanced by divergence aloft that produces a vorticity sink through

the stretching term. This divergence of mass at upper levels requires an upward velocity in this region and, thus, mass convergence near the surface that maintains the vorticity anomaly against friction via stretching. The eddy vorticity flux convergence at upper levels thus acts to sustain the vorticity anomaly against surface drag, increasing the persistence of the NAO anomaly.

To complete the feedback loop, we must show that the secondary circulation induced by the convergence of eddy vorticity flux at upper levels produces conditions favorable to eddy growth. This is the case since the adiabatic cooling due to the vertical circulation cools in the right locations to offset eddy heat fluxes and maintain thermal wind balance associated with the vorticity anomalies. Thus, the baroclinicity in the region of the vorticity anomaly is enhanced, as is the generation of eddies. The vertical motion that we associate with the convergence due to the stretching term is equivalent to Ekman pumping in Robinson’s (2006) argument for why eddy-driven jets can be self-sustaining. If the eddies associated with the jet propagate meridionally away from the region of strongest baroclinicity before breaking, one expects a stronger equilibrium temperature gradient from the weakened heat transport by the residual circulation (Hartmann 2007). The increased baroclinicity in this region generates more eddies, which act to sustain the jet.

Evidence of this mechanism can be found in previous studies such as Holopainen and Oort (1981), where they found that transient eddies maintain the North Atlantic low against the dissipative effects of surface friction. Similarly, Lau and Nath (1991) showed that forcing of the monthly-mean geopotential height field by the synoptic transient-eddy vorticity fluxes at upper levels balances (and are actually stronger than) the opposing tendencies due to eddy heat fluxes, whereas at lower

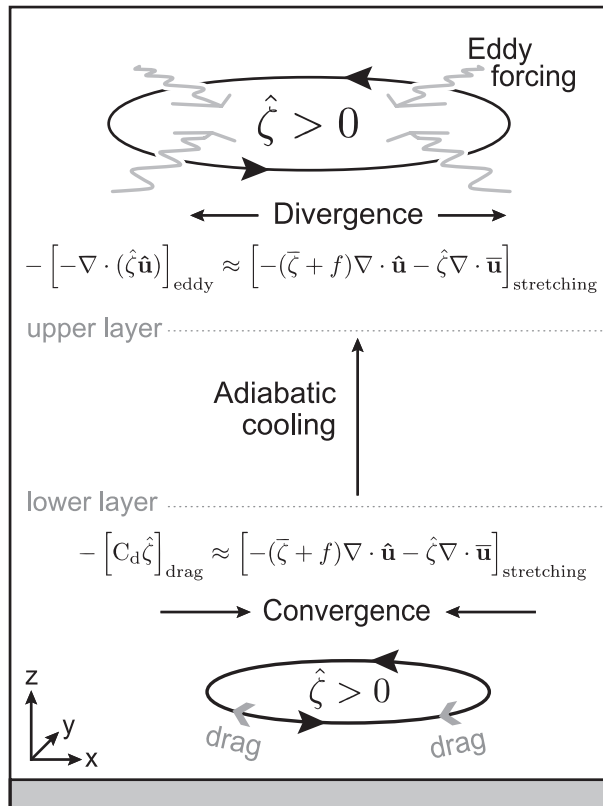


FIG. 3. A schematic of the 3D eddy feedback mechanism for a positive vorticity anomaly. Straight black arrows represent the large-scale circulation cell set up to balance the upper-level convergence of eddy vorticity flux (wavy arrows) and counter the dissipation of the low-level vorticity anomaly by surface drag (drag coefficient  $C_d$ ). The adiabatic cooling associated with the vertical motion balances the low-level temperature advection, maintaining the temperature gradient. This mechanism represents a positive feedback since the vorticity anomalies organize the upper-level eddies, which act to sustain the anomalies.

levels the two effects reinforce one another. Feldstein (1998) found that high-frequency eddies extend the lifetime of a low-frequency anomaly in a GCM and that the anomaly’s decay is regulated by the stretching term. Later, he demonstrated, using a reanalysis dataset, that the growth of the anomalous circulation associated with the NAO is driven by the eddy fluxes and that the divergence term is a major contributor to the NAO’s subsequent decay (Feldstein 2003).

**6. Vorticity–eddy feedback of the NAO**

In a zonal-mean, vertically averaged framework, LH01 found that the zonal index and its eddy forcing closely follow the differential equation

$$\frac{dz}{dt} = m - \frac{z}{\tau}, \tag{3}$$

where  $m$  is the zonal-mean eddy-forcing time series,  $z$  the index of the annular mode, and  $\tau$  a decay time scale. In this section, we quantify the feedback between the NAO and eddy forcing using the formalism of LH01, but applied to the local 3D structure of the NAO.

*a. NAO forcing patterns*

The analysis described utilizes mass-weighted upper- and lower-level fields, averaged for levels 300, 250, 200, and 150 mb and 1000, 925, and 850 mb, respectively. The following results are robust in that pairing any upper and lower level and performing the analysis produces similar conclusions (results not shown). Analysis at pressure levels in the midtroposphere reveals weak/insignificant feedbacks owing to the weakness of the divergence there.

The three-dimensional NAO structure is not entirely barotropic, and the structure in the upper troposphere differs from that at the surface where surface drag damps the anomalies (cf. Figs. 2b,c). Because the proposed mechanism requires that the upper-level transient eddy vorticity flux convergence offset dissipation of the lower-level anomaly by surface drag, the lower-level anomaly structure is critical in diagnosing a positive feedback. If the upper-level eddy forcing pattern aligns with the lower-level NAO vorticity structure, we infer that a secondary circulation has been set up in such a way that the upper-level fluxes maintain the lower-level anomaly against frictional dissipation (Fig. 3).

In support of this mechanism, Fig. 4a shows the NAO structure of the mass-weighted, upper-level stretching term. In the midlatitudes, the upper-level stretching pattern organizes over the eastern Atlantic basin and Spain, similar to the lower-level NAO structure in Fig. 2c, although of opposite sign. We have confirmed that the lower-level divergence over the eastern Atlantic (not shown) induces a negative vorticity tendency, which sustains the negative vorticity anomaly against drag. In the higher latitudes over Greenland, the stretching term is in quadrature with the lower-level NAO vorticity structure. The linear wave forcing pattern associated with the NAO is organized similarly to the stretching field (Figs. 4a,b) although of opposite sign. This relationship is consistent with baroclinic wave theory where vortex stretching by the divergent secondary circulation balances the effect of shear on the advection of vorticity (Holton 2004). In the north lobe over Greenland, the stretching field contributes to upstream propagation of the NAO anomaly while the linear wave terms tend to advect the anomaly downstream, reminiscent of a propagating Rossby wave (Holton 2004). We will show that the midlatitude NAO anomaly exhibits a positive feedback with the transient eddies while the northern

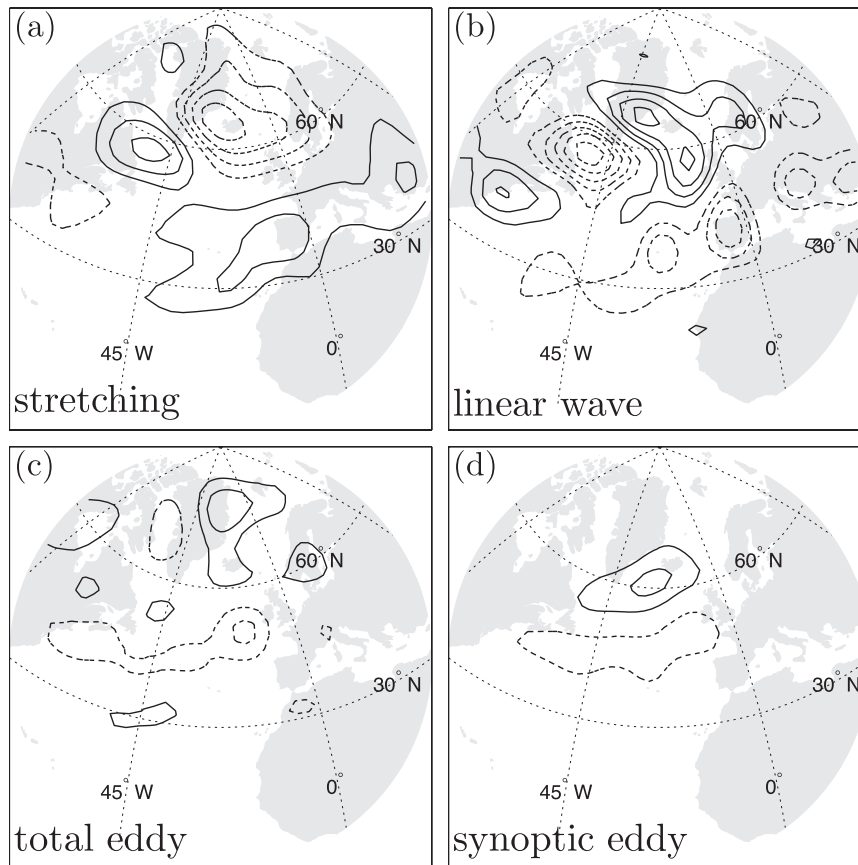


FIG. 4. NAO structures of (a) the upper-level stretching term, (b) the linear wave term, (c) total eddy forcing, and (d) synoptic eddy forcing obtained by regressing  $Z(t)$  onto the field. Contours are drawn every  $3 \times 10^{-11} \text{ s}^{-2}$  with negative contours dashed and the zero contour line omitted.

anomaly shows no such feedback and is dominated by a propagating Rossby wave.

Figure 4c depicts the total eddy-forcing pattern. This field exhibits convergence of eddy vorticity flux in the polar regions and divergence in the midlatitudes, consistent with Fig. 3. Previous authors have shown the importance of the high-frequency eddies in driving and maintaining large-scale variability in the atmosphere (Nakamura and Wallace 1990; Branstator 1992; LH01; Feldstein 2003; Eichelberger and Hartmann 2007). Robinson (1991) found evidence of a feedback between synoptic waves and vorticity anomalies in a simple GCM and concluded that the eddies both reinforce the low-frequency structures as well as slow their eastward propagation. We separate the “synoptic” (high-frequency) eddy forcing from the total forcing by high-pass ( $< 7$  day) filtering the anomalous horizontal winds ( $\mathbf{u}'$ ) and the vorticity ( $\zeta'$ ) and computing the component of the eddy forcing due to fluctuations on these synoptic time scales  $[-\nabla \cdot (\zeta' \mathbf{u}')]$ . The resulting regression (Fig. 4d) of the

NAO time series onto the synoptic eddy forcing aligns well with the upper-level NAO vorticity structure (Fig. 2b), supporting the hypothesis that the synoptic eddies are acting to sustain the large-scale NAO structure. We quantify this argument in the next section.

Finally, note that while the stationary wave forcing is the same order of magnitude as the other terms, it is nearly constant in time and thus will be neglected in our temporal correlation analysis.

#### b. Definition of forcing time series

We project the eddy forcing field onto the lower-level NAO vorticity pattern to obtain the forcing time series  $M(t)$ , which we have normalized to have a standard deviation of one (note that  $M$  has zero mean by construction). By defining the forcing time series  $M(t)$  in this way, we have implicitly assumed that the optimal shape of the eddy vorticity convergence for forcing the NAO anomaly is the shape of the NAO vorticity anomaly itself. It is not obvious that the best way to force an

anomaly is to use in-phase forcing since advection is present. The following heuristic argument suggests why this may be appropriate for a steady Rossby wave.

Consider the stationary vorticity equation for a simple background zonal flow:

$$\bar{u} \frac{\partial \hat{\zeta}}{\partial x} + \beta \hat{v} = S - \alpha \hat{\zeta}. \quad (4)$$

Here, drag is parameterized as a linear function of the anomalous vorticity and  $S$  represents a vorticity source. Defining the streamfunction  $\psi(x)$  as  $\zeta = \nabla^2 \psi$  and decomposing into Fourier components using  $\psi(x, y) = \tilde{\psi}(k, l)e^{i(kx+ly)}$  and looking at the resonant mode where  $\bar{u} = \beta(k^2 + l^2)^{-1}$ , one can obtain

$$\tilde{\psi} \sim \frac{-\tilde{S}}{\alpha(k^2 + l^2)}, \quad \tilde{\zeta} \sim \frac{\tilde{S}}{\alpha}. \quad (5)$$

Therefore, under the assumption that the wave is approximately stationary and resonant, it is plausible that in-phase forcing will efficiently reinforce the wave. Further analysis of this question is beyond the scope of the present work.

We project the upper-level vorticity onto the lower-level NAO vorticity pattern, calling the resulting time series  $Y(t)$ . This time series captures the structure within the upper-level vorticity pattern that can best balance the low-level drag. A positive feedback requires that the lower-level NAO vorticity anomaly be sustained by the upper-level eddy forcing. Thus, our hypothesis implies that

$$\frac{dY}{dt} = M - \frac{Y}{\tau}, \quad (6)$$

where  $\tau$  is the decay time scale and  $M$  is composed of both a random forcing component and a component organized by the low-frequency vorticity anomalies.

*c. Feedback analysis*

Figure 5a shows the cross-correlation between  $M$  and  $Y$  for the Atlantic region, with positive lags signifying that  $Y$  leads  $M$ . The greatest correlations occur at negative lags, consistent with the low-frequency anomalies being driven primarily by random fluctuations of the eddies as described by (6). However, positive correlations at positive lags larger than the time scale of a typical synoptic disturbance (7 days) imply a positive feedback between the eddy forcing and the slowly varying vorticity field. The total eddy forcing time series is positively correlated with  $Y$  at the 95% confidence level for lags +5 to +11 days (see appendix A for details). Although the cross-correlations are small, they are consistently

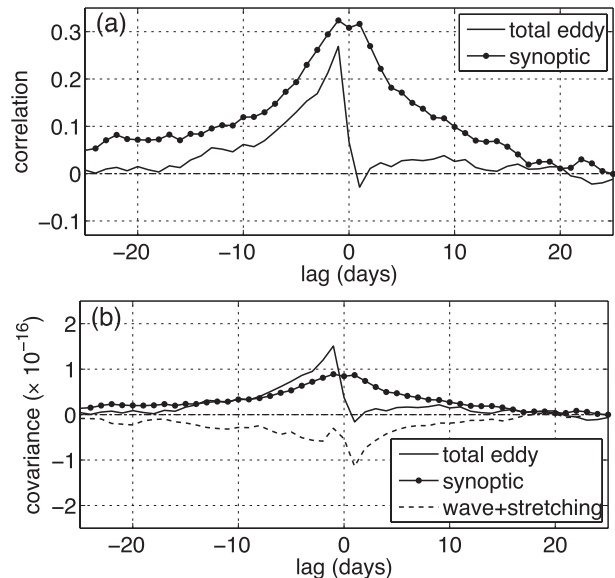


FIG. 5. (a) Cross-correlations between  $Y$  and  $M$  in the Atlantic region for the total eddy forcing (solid) and synoptic eddy forcing (circles). (b) Cross-covariances between  $Y$  and the forcing time series for the total eddy forcing (solid), synoptic eddy forcing (circles), and the linear wave term plus stretching term (dashed) in units of  $s^{-3}$ . In both panels, positive lags imply that  $Y$  (vorticity) leads the eddy forcing.

positive over a long period of time and so have a significant effect, as in the zonal-mean case (LH01; LH03). These positive correlations support the hypothesis that the NAO anomalies organize the eddy fluxes for self-maintenance.

One might argue that the positive correlations at positive lags are due purely to the memory of the eddies themselves and are not a reflection of the NAO anomalies organizing the eddies. To confirm that this is not the case, we repeat the correlation analysis for the synoptic eddy forcing only  $[-\nabla \cdot (\zeta' \mathbf{u}')$ , with the resulting cross-correlations shown in Fig. 5a. It is clear from this curve that the synoptic eddies act to sustain the NAO vorticity anomalies at large positive lags and, indeed, they are the main source of the positive correlations in the total eddy field with the nonsynoptic eddies playing a dissipative role (infer by subtraction). Since the synoptic eddies fluctuate on time scales shorter than 7 days and yet they account for the positive correlations at lags up to +20 days, the vorticity structure must be organizing the synoptic eddies. Hence, the net positive feedback between the eddies and the NAO vorticity anomalies is driven by the high-frequency eddy fluxes.

It could be argued that the positive eddy feedback is small compared to the effects of the linear wave term and the stretching term (2). To show the importance of the eddy terms with respect to all of the others in the vorticity

tendency equation, we plot the cross-covariance of  $Y$  with the forcing time series of the total eddy term, the synoptic eddy term, and the sum of the stretching term and the linear wave term in Fig. 5b. The synoptic eddy forcing contributes substantially to the total vorticity forcing at all lags, and the total eddy forcing is a similar magnitude of the other forcing terms at lags beyond +5 days.

#### d. Importance of feedback in the midlatitudes

Applying the previous analysis to the north and south lobes individually (as defined in Figs. 2b,c), Fig. 6a shows that only the south (midlatitude) lobe of the NAO exhibits a positive feedback. Here, correlations for the south lobe between 0 to +16 days lie above the 95% confidence level while only day +9 satisfies this criterion in the north lobe. This result appears robust to the region definitions, although increasing the south lobe region much beyond the scale of the surface vorticity anomaly causes the correlations to fall below the calculated confidence level (owing to an increase of locations not encompassed by the NAO anomaly).

The difference between the two lobes can also be seen in the cross-covariances between the vorticity anomalies and the different forcings shown in Figs. 6b,c. The correlations associated with the linear wave term in the north lobe suggest a propagating wave, with positive correlations prior to lag 0 and equally strong negative correlations after lag 0. In the south lobe, the linear wave term projects positively onto the NAO structure at positive lags, consistent with the induced secondary circulation associated with the eddy feedback. These spatial relationships were also seen in Fig. 4b. In addition, Figs. 6b,c demonstrates that the feedback mechanism, whereby the upper-level convergence of eddy vorticity flux counters the anomalous large-scale upper-level divergence, is present in the midlatitudes but not over Greenland.

These findings suggest that, while the midlatitude anomaly is self-sustaining due to a positive eddy feedback, the northern anomaly behaves like a propagating upper-level Rossby wave. This difference can be understood by the size of the NAO lobes. The northern anomaly is the correct size to capture the variability associated with Rossby waves. Thus, the definition of the NAO picks out the jet shift in the midlatitude region and Rossby wave propagation in the northern lobe.

#### e. Estimation of feedback strength in the south lobe

If  $Y$  and  $M$  are linearly related according to (6), then the decay time scale  $\tau$  can be obtained by converting to Fourier space and using basic cross-spectrum analysis techniques. Letting  $\mathcal{Y}$  and  $\mathcal{M}$  denote the Fourier transforms of  $Y$  (upper-level vorticity projected onto the

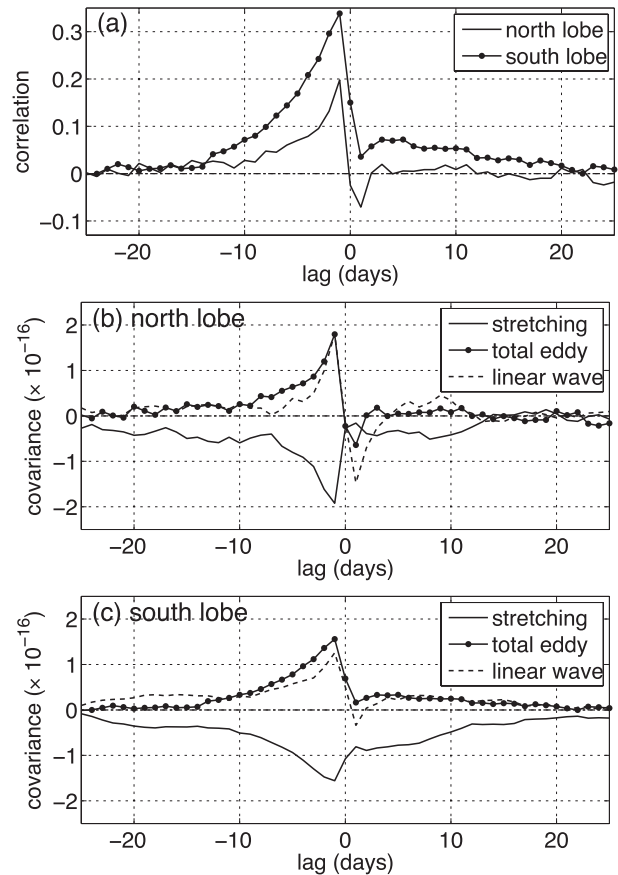


FIG. 6. (a) Cross-correlations between  $Y$  and the total eddy forcing time series  $M$  for the south lobe and north lobe separately. (b),(c) Cross-covariances between  $Y$  and the forcing time series for the stretching term (solid), total eddy forcing (circles), and linear wave forcing (dashed) for the north and south lobes in units of  $s^{-3}$ . In all panels, positive lags imply that  $Y$  (vorticity) leads the eddy forcing.

lower-level pattern) and  $M$  (eddy forcing time series) respectively, the transfer function between  $Y$  and  $M$  can be written as

$$\frac{\mathcal{M}(\omega)\mathcal{Y}^*(\omega)}{\mathcal{Y}(\omega)\mathcal{Y}^*(\omega)} = \frac{1}{\tau} + i\omega, \quad (7)$$

where  $\omega$  denotes the angular frequency and the asterisk signifies the complex conjugate. This equation is obtained by taking the Fourier transform of (6), rearranging terms, and multiplying by  $\mathcal{Y}^*$ . Figure 7a shows the real and imaginary parts of (7) for the south lobe since this region shows evidence of a feedback. The real part of the transfer function is approximately constant up to a frequency of  $0.05 \text{ days}^{-1}$ , while at higher frequencies noise starts to dominate. The imaginary part of the transfer function follows the angular frequency [as

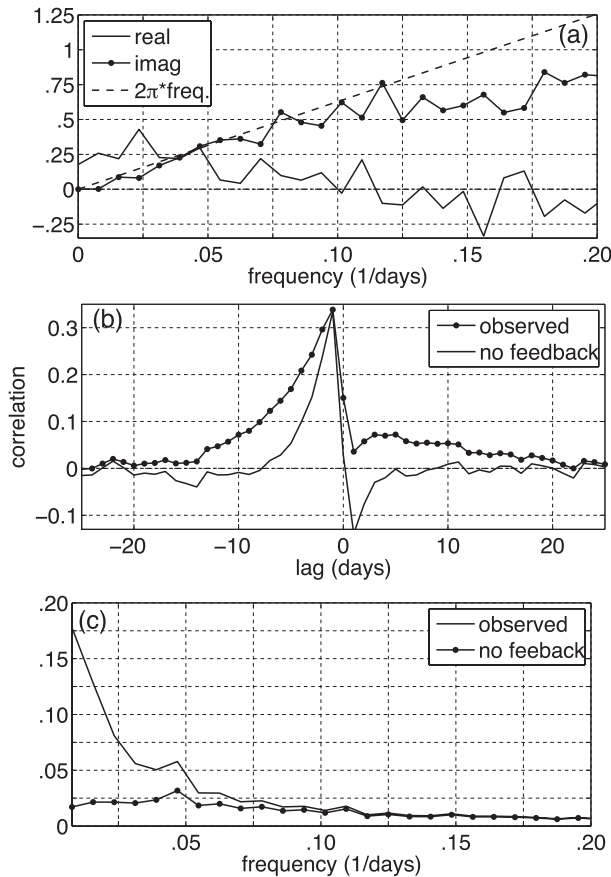


FIG. 7. (a) The real and imaginary parts of the transfer function of  $Y$  and  $M$  for the south lobe. The angular frequency curve (dashed) denotes the imaginary part predicted by linear theory. (b) The cross-correlation between  $Y$  and  $M$  in the south lobe as observed and with the estimated feedback removed. (c) The power spectrum of  $Y$  observed and with the feedback removed ( $\tilde{Y}$ ).

predicted by the second rhs term of (7)] up to a frequency of about  $0.125 \text{ days}^{-1}$ . Given that our calculated transfer function follows the predicted behavior of (7) for low frequencies below  $0.05 \text{ day}^{-1}$ , we follow the method outlined in LH01 (see their appendix A) and use these curves to estimate the decay time scale  $\tau = 3.5$  days. This time scale represents the  $e$ -folding time of the time series  $Y$  if the eddies did not force the NAO anomaly. LH03 followed this same method and calculated a decay time scale of 6.8 days for the Northern Hemisphere annular mode calculated from zonal-mean data. The fact that our calculated time scale is about half as long as that of LH03 indicates that the zonal-mean, hemispheric mode would persist longer than the regional NAO in the absence of a feedback. This difference makes intuitive sense since a zonally symmetric structure cannot decay by zonal propagation while a zonally localized pattern can.

We can quantitatively estimate the strength of the eddy feedback in the south lobe of the NAO under the assumption that the eddy forcing produced is proportional to the vorticity anomalies. Following LH01, we model the eddy-forcing time series  $M$  such that

$$M = \tilde{M} + bY, \tag{8}$$

where  $\tilde{M}$  is a random forcing and  $b$  denotes the feedback strength between the forcing and the vorticity anomalies. A semianalytic derivation of this simple linear relationship between a low-frequency anomaly and anomalous eddy flow can be found in Jin et al. (2006). Following the method outlined by LH01 (see their appendix C), the feedback strength  $b$  [see (8)] is found to be 0.21 in the south lobe. In terms of decay time scales, it can be shown (the LH01 appendix C) that the feedback extends the damping time scale as  $\tau \rightarrow \tau/(1 - b\tau)$ , or in the case of the south lobe of the NAO, from 3.5 days to 13.2 days.

The feedback strength  $b$  is used to compute the cross-correlations between  $\tilde{M}$  and  $\tilde{Y}$  as well as the power spectrum of  $\tilde{Y}$  without feedback (Figs. 7b,c). By construction in the calculation of  $b$ , the cross-correlations at positive lags drop to zero in the case of no feedback. The power spectra of  $Y$  and  $\tilde{Y}$  (Fig. 7c) indicate that the power at low frequencies is greatly reduced with the removal of the feedback, indicating that the feedback between the synoptic eddies and the anomaly accounts for much of the persistence of the NAO anomalies in the midlatitudes. Comparing the no-feedback correlations (Fig. 7b) with the correlations in the north lobe (Fig. 6b), we see that both exhibit near-zero correlations by +5 days and behave similarly at both positive and negative lags, indicating that the north lobe lacks a positive eddy feedback.

### 7. Asymmetry between phases of the NAO

Nakamura and Wallace (1991) documented the skewness of the 500-mb geopotential height field, a statistic denoting the asymmetry of the frequency distribution about the mean. They plotted the skewness of the anomalous 500-mb geopotential height field at every location and found a region of positive skewness poleward of the Atlantic storm track and a region of negative skewness equatorward, a “high over low” structure similar to that of the low-phase NAO. Rennert and Wallace (2009) suggested that the skewness in the 500-mb geopotential height field results from the coupling between the variability on intermediate (6–30 days) and long (30+ days) time scales. Consistent with these results, Woollings et al. (2008, 2010) highlighted the robust nature of the well-known negative skewness of the NAO time series. A

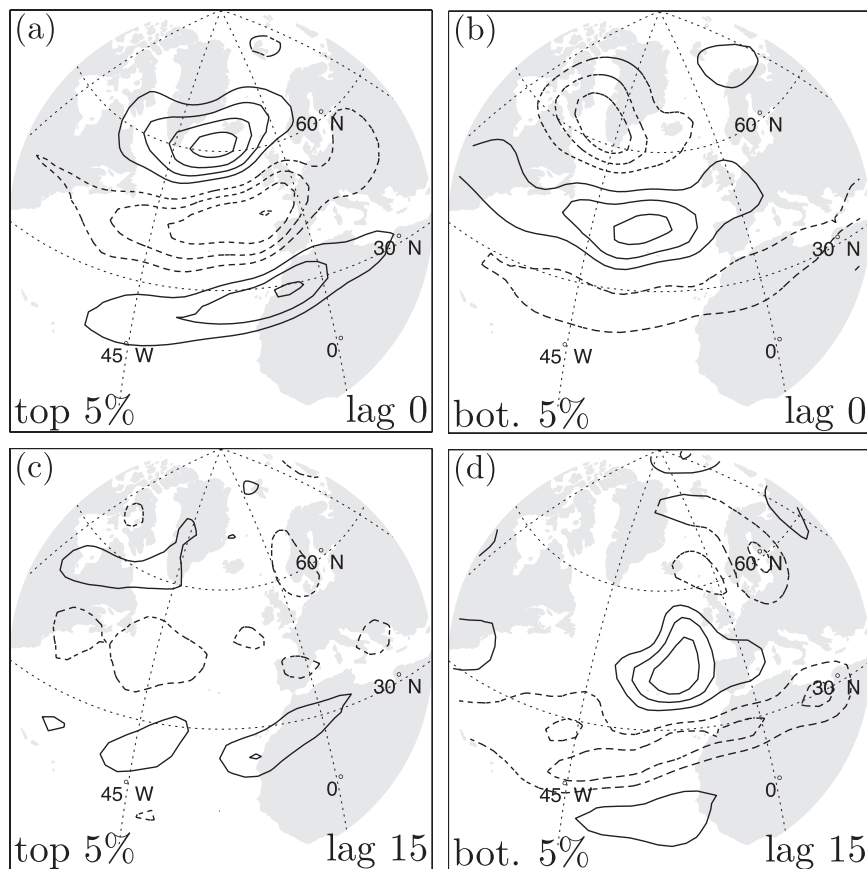


FIG. 8. Lag 0 days patterns of upper-level relative vorticity for the (a) top and (b) bottom 5% of the NAO index  $Z$ . (c),(d) Lag 15 patterns of the same fields as in (a) and (b). Contours in the top (bottom) panel are drawn every  $6.25 (3) \times 10^{-6} \text{ s}^{-1}$  with negative contours dashed and the zero contour line omitted.

negative skewness ( $-0.19$  for our  $Z$ ) implies more extreme negative values than positive and more positive values than negative overall. Woollings et al. (2010) demonstrated significantly more low-phase NAO events (when the NAO index is below  $-1$ ) lasting 10–14 days than would be expected by a simple AR1 model, with high-phase NAO events behaving more similarly to an AR1 process, supporting their synoptic view.

In this section, we present a simple measure of the persistence of the NAO phases and show that the low phase has longer persistence than the high phase. Applying our eddy-feedback analysis to each phase individually, we find a stronger positive eddy feedback for the low phase than the high phase, consistent with the extended persistence of the low phase.

#### a. Persistence of NAO phases

Compositing the upper-level vorticity field on days when  $Z$  falls into its upper 5% or lower 5% shows a remarkable difference between the two phases. Figure 8 displays these composites at the NAO peak (lag 0 days)

and 15 days later. At lag 0 days, the high-phase and low-phase structures are very similar, although 180 degrees out of phase. However, at a lag of +15 days, the low-phase NAO structure strongly resembles that at lag 0 days, while the high-phase NAO structure appears significantly weaker and less organized. Similar results emerge when we composite the zonal winds, sea level pressure, and geopotential height fields at upper levels at large lags. This raises the question whether the low phase of the NAO has a significantly greater persistence than the high phase.

To explore the persistence of the difference phases, we follow Woollings et al. (2010) and define a run statistic for the different phases of the NAO. The duration of a high-phase (low-phase) NAO event is defined by the number of consecutive days  $Z$  is above (below)  $+1$  ( $-1$ ). Instead of plotting the number of runs as done by Woollings et al. (2010), we analyze the frequency of events with durations equal to or exceeding  $n$  days, defined as the number of runs normalized by the total number of distinct events in the associated phase [223 (137) events for

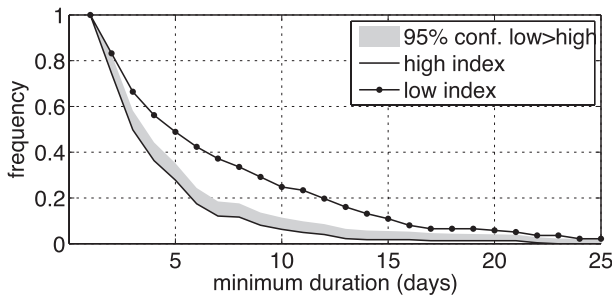


FIG. 9. Frequency of NAO events that last *at least* a certain number of days. A high- (low-) phase event is defined for values above (below) +1 (−1). Shading denotes the 95% confidence range that the low-index phase is significantly more persistent than the high phase (see appendix B for details).

the high (low) phase]. We choose to analyze frequency instead of total counts since we are not interested in whether the total number of events is different between phases but only whether low-phase events persist longer. Figure 9 displays the results, where the gray shading denotes the 95% confidence limit that low-phase events more frequently last at least  $n$  days compared to high-phase events (see appendix B for calculations). We find that significantly more events have minimum durations of 2–27 days for the low phase than the high phase, consistent with Fig. 8. Our results differ from those of Woollings et al. (2010) in that we state that, even if the two phases of the NAO behave as AR1 processes, they are *different* AR1 processes.

It is important to note that the skewness of  $Z$  alone is not an appropriate measure of an asymmetry in persistence. While a negative skewness is consistent with the low-phase NAO having more extreme, longer-lasting events, it is a measure of event amplitude only. The persistence is a measure of the magnitude and duration of a given event, where ordering in time matters. It is for this reason that we investigate the difference in persistence using a duration statistic and not the skewness alone.

*b. Feedbacks of the high- and low-phase NAO*

We have established that low-phase NAO events persist for longer periods of time than high-phase events. Could this asymmetry in persistence be due to a difference in eddy feedback strength? To address this question, we separate  $Z$  into a high ( $Z_+$ ) and low ( $Z_-$ ) index in the following way:

$$\begin{aligned}
 Z(t)_+ &= \begin{cases} Z(t) & \text{if } Z(t) > 0 \\ 0 & \text{otherwise,} \end{cases} \\
 Z(t)_- &= \begin{cases} Z(t) & \text{if } Z(t) < 0 \\ 0 & \text{otherwise.} \end{cases}
 \end{aligned}
 \tag{9}$$

For notational clarity, we will define  $t_+$  as the vector of days when  $Z_+ \neq 0$  and likewise  $t_-$  as the vector of days when  $Z_- \neq 0$ . The resulting  $t_+$  contains 2736 days and  $t_-$  contains 2478 days.

We wish to apply the same method as in previous sections to investigate a positive feedback between the eddy forcing and the two phases of the NAO. We define the lower-level high- (low-) phase NAO pattern as the regression of  $Z_+$  ( $Z_-$ ) onto the lower-level daily relative vorticity. As one might expect, the two patterns are nearly identical but of opposite sign (not shown). As before, we wish to compare the upper-level vorticity field with the lower-level NAO response; thus,  $Y_+(t)$  [ $Y_-(t)$ ] is defined as the projection of the upper-level relative vorticity on days  $t_+$  ( $t_-$ ) onto the high- (low-) phase NAO pattern.

Last, we must define the eddy forcing time series for the different phases. Since one expects the response of the eddy forcing to lag the large-scale circulation (as seen in the full NAO feedback case), we cannot simply define the eddy forcing time series on days  $t_+$  and  $t_-$ . Rather,  $M_+(t)$  [ $M_-(t)$ ] is defined as the projection of the upper-level eddy forcing field onto the lower-level high- (low-) phase pattern for *all* days. The forcing time series  $M_+(t)$  and  $M_-(t)$  are correlated at  $-0.96$ . This high correlation is expected since the NAO structures at lower levels for the high and low phases are nearly identical in shape.

Figure 10 shows the cross-correlations between  $M_+$  and  $Y_+$  and between  $M_-$  and  $Y_-$  in the south lobe. At positive lags, the low-phase correlation is statistically different from zero for lags 0 to +14 days at 95% confidence. The high-phase correlation is significant only at lags of +3 to +7 days and, hence, lacks the positive eddy feedback beyond a single eddy lifetime. To confirm that the synoptic (high-frequency) eddies contribute to this asymmetry, Fig. 10b shows the cross-covariances between the NAO time series and the synoptic eddies and between the NAO time series and the stretching term for the two phases. We have verified that the non-synoptic eddies contribute similar magnitudes for both phases, implying that the asymmetry in the total eddy forcing is due purely to the synoptic eddy component. Consistent with our proposed feedback mechanism, the stretching term negatively forces the vorticity anomalies at upper levels for both phases, thus positively forces the vorticity anomalies at lower levels. Plots of correlation (not shown) show similar results, implying that the differences in Fig. 10b are not merely due to a difference in variance between the two phases.

To investigate the reason for the apparent asymmetry in feedback between the two NAO phases, we compute the vector  $\mathbf{E} = (v'^2 - u'^2, -u'v')$ , which corresponds to

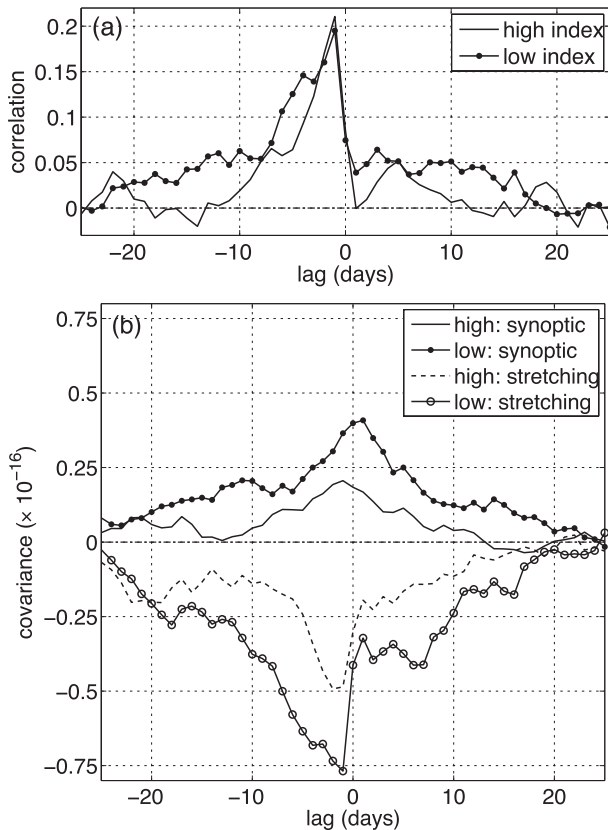


FIG. 10. (a) Cross-correlations in the south lobe between the total eddy forcing time series ( $M_+$ ,  $M_-$ ) and the vorticity anomaly time series ( $Y_+$ ,  $Y_-$ ) for the high and low indices of the NAO, respectively. (b) Cross-covariances in the south lobe between the high- and low-index NAO time series and the forcing due to the synoptic eddies as well as the forcing due to the stretching term in units of  $s^{-3}$ . Positive lags imply that  $Y$  (vorticity) leads the forcing.

the horizontal components of the high-frequency  $\mathbf{E}$  vector defined by Hoskins et al. (1983). The vector may be interpreted as an effective momentum flux, and its horizontal divergence gives the forcing of the background flow by the synoptic eddies. We composite the horizontal  $\mathbf{E}$  vectors and the vertically averaged zonal wind for the top and bottom 5% of the NAO index  $Z$  and plot the result in Fig. 11. The high-phase composite wind shows a clear poleward shift of the jet, whereas an equatorward shift of the jet is evident in the low-phase. A remarkable difference between the two phases is the location and direction of the eddy propagation away from the jet. In the low phase, the eddies turn preferentially poleward over the mid-Atlantic, in the NAO region. In the high phase, the eddies propagate along the axis of the jet and then break equatorward over eastern Europe, downstream of the NAO. Figure 11 implies that the eastward propagation of the synoptic eddies is

blocked during the low-phase NAO, unlike in the high phase when the eddies break in a broad region downstream of the Atlantic. This figure is consistent with the PV streamer analysis of Martius et al. (2007), who show that during the high phase of the NAO most wave breaking is of the LC1 type and occurs downstream and equatorward of the jet, while the low phase exhibits wave breaking of LC2 type and poleward of the jet (see Benedict et al. 2004; Frankze et al. 2004 for additional references).

The cross-correlation and  $\mathbf{E}$ -vector plots in Figs. 10 and 11 demonstrate the greater synoptic eddy feedback found during the low-phase NAO. We argue that, although the magnitude of the eddies (length of  $\mathbf{E}$  vectors) during the low phase is small in comparison to those of the high phase, their propagation due to the weak flow associated with the low-phase NAO better aligns and reinforces the NAO anomaly. The wave breaking associated with the high-phase NAO occurs too far downstream to reinforce the existing NAO anomaly.

## 8. Summary

Analysis of the vorticity tendency equation in the upper troposphere and near the surface has demonstrated that a positive feedback exists between the eddies and vorticity anomalies associated with the NAO. At upper levels the convergence (divergence) of synoptic eddy-vorticity flux counteracts the effects of the large-scale divergence (convergence). At lower levels the large-scale convergence (divergence) associated with the induced vertical circulation cell reinforces the lower-level NAO anomaly and sustains the anomaly against frictional drag. The inferred adiabatic cooling associated with the rising motion in the vorticity maximum sustains the thermal structure of the NAO anomaly, enhancing the baroclinicity and thus eddy generation, completing the feedback loop. Our proposed feedback mechanism is consistent with that of a self-sustaining jet, as discussed by Robinson (2006), where the cooling and warming due to mean vertical motion offset the eddy heat flux anomalies.

While the linear wave term projects well onto the NAO anomaly in midlatitudes, the field is in quadrature with the northern anomaly over Greenland. Our analysis suggests that the persistence of the NAO in the midlatitudes can be explained by a positive eddy feedback, while the north lobe has no feedback with the eddies and acts as a propagating Rossby wave. The lack of feedback in the lobe over Greenland and presence of feedback in the midlatitude lobe can be understood by

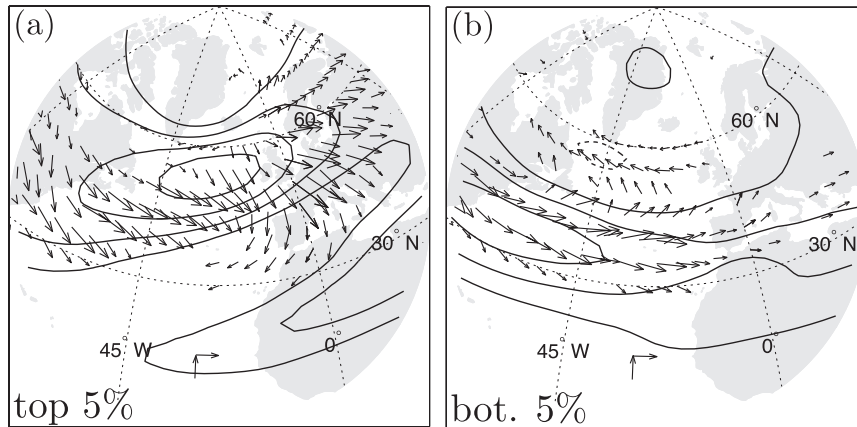


FIG. 11. Composites of vertically averaged horizontal  $\mathbf{E}$  vectors (arrows) and the vertically averaged zonal wind (contours) for the (a) top 5% and (b) bottom 5% of the NAO index  $Z$ . Contours are drawn every  $5 \text{ m s}^{-1}$  with negative contours dashed. The reference vectors have magnitudes of  $20 \text{ m}^2 \text{ s}^{-2}$ . The zero contour line has been omitted.

the relative sizes of the two anomalies. The southern anomaly has a longer zonal extent than the northern anomaly. The domain of the northern anomaly is the correct size to capture Rossby wave variability while the midlatitude lobe captures the jet shift.

The NAO is often viewed as a linear oscillation/shift of the jet stream to its north and south, but we have shown that low-phase NAO events last significantly longer than high-phase NAO events. In other words, once the jet has shifted equatorward and is more zonally oriented, it stays in this configuration for longer periods of time than when it is poleward of its climatological position. Applying our eddy feedback framework to this asymmetry, we demonstrated that the low-phase NAO exhibits a larger eddy feedback than the high phase, consistent with its extended persistence. Composites of vertically averaged, high-frequency  $\mathbf{E}$  vectors for the two phases show the difference in eddy propagation in the midlatitudes. The eddies in the high phase do not reinforce the NAO anomaly as much because of their extended downstream propagation, while the weak zonal flow associated with the low-phase NAO induces the eddies to break in the region of the anomaly, reinforcing the NAO pattern.

*Acknowledgments.* We thank John M. Wallace and Dargan Frierson for their helpful suggestions and Randal J. Barnes for his aid in developing the statistical framework. We would also like to thank the three reviewers for their help in greatly improving the clarity of this manuscript. This work was supported by the Climate Dynamics Program of the National Science Foundation under Grant ATM 0409075.

## APPENDIX A

### Cross-Correlation Statistics

We define  $\hat{\rho}(h)$  as the estimated cross-correlation between the two time series  $Y$  and  $M$ , each composed of  $W = 43$  winter seasons of  $d = 121$  days each. To simplify the formulas, we let  $Y = Y(d, w)$ , which denotes the  $d$ th day of the  $w$ th winter season. Then,  $\hat{\rho}$  is estimated by

$$\hat{\rho}(h) = \frac{\sum_{w=1}^{43} \sum_{d=1}^{121-h} [Y(d, w) - \mu_Y][M(d + h, w) - \mu_M]}{43(121 - h)\sqrt{\nu_Y(h)\nu_M(h)}}, \quad (\text{A1})$$

where  $\mu_Y$  and  $\mu_M$  are the arithmetic averages of  $Y$  and  $M$  over all winter days, and  $\nu_Y(h)$  and  $\nu_M(h)$  are the estimated variances at lag  $h$ , defined by

$$\nu_Y(h) = \frac{1}{43(121 - h)} \sum_{w=1}^{43} \sum_{d=1}^{121-h} [Y(d, w) - \mu_Y]^2 \quad (\text{A2})$$

and

$$\nu_M(h) = \frac{1}{43(121 - h)} \sum_{w=1}^{43} \sum_{d=1}^{121-h} [M(d + h, w) - \mu_M]^2. \quad (\text{A3})$$

Note that if the cross-correlations were normalized by  $(43 \times 121)^{-1}$ ;  $\mu_Y = \mu_M = 1$  by construction.

The method to assess the statistical significance of the cross-correlations directly follows that outlined by LH01.

We perform a Monte Carlo simulation to test the following null hypothesis: the cross-correlation is zero at positive lags. We generate 1000 random forcing time series  $\hat{M}$  (5214 days each split into 121-day seasons) using a moving average model with parameters  $\theta_i$ . These parameters are estimated from the autocorrelation of the real forcing time series  $M$  up to lag 6 (where the autocorrelation drops to near zero) using the iterative method outlined by Box et al. (2008). We calculate the corresponding  $\hat{Y}$  (model time series of  $Y$ ) using (6) with the complimentary  $\tau = 3.5$  days (see appendix A of LH01). Calculating the cross-correlations for each of the 1000 sets of  $\hat{M}$  and  $\hat{Y}$  and computing the 95th percentile correlation at positive lags gives a 95% significance value of 0.023.

## APPENDIX B

### Statistical Significance of Duration

We model the NAO time series  $Z$  as a strictly stationary, zero-mean, AR1 process with parameters  $\phi$  and  $\sigma$  (Box et al. 2008). The model time series  $\hat{X}$  has 43 chunks of 121 days each (similar to  $Z$ ). Although the NAO time series  $Z$  has zero mean, each winter-mean NAO index is *not zero*. Thus, we adjust our model time series to incorporate nonzero seasonal-mean values and denote this final model time series as  $X$ . Letting  $d$  denote the day within a winter season,  $w$  the specific winter season, and  $\mathcal{W}(w)$  the mean-seasonal value estimated from the  $w$ th season of  $Z$ , we obtain

$$\hat{X}(d, w) = \phi \hat{X}(d - 1, w) + \epsilon(d) \quad (\text{B1})$$

and

$$\begin{aligned} X(d, w) &= \hat{X}(d, w) + \mathcal{W}(w) \\ &= \phi \hat{X}(d - 1, w) + \epsilon(d) + \mathcal{W}(w), \end{aligned} \quad (\text{B2})$$

where  $\epsilon$  is white noise with variance  $\sigma$ . To estimate the parameters  $\sigma$  and  $\phi$  from the data, a modified NAO time series is defined:

$$\hat{Z}(d, w) \equiv Z(d, w) - \mathcal{W}(w). \quad (\text{B3})$$

Using  $\hat{Z}$ , we estimate the AR1 parameters:

$$\phi = \frac{\sum_{w=1}^{43} \sum_{d=2}^{120} \hat{Z}(d - 1, w) \hat{Z}(d, w)}{\sum_w \sum_d \hat{Z}(d, w)^2} \quad (\text{B4})$$

and

$$\sigma^2 = \frac{1}{(43 \times 120)} \sum_{w=1}^{43} \sum_{d=2}^{121} [\hat{Z}(d - 1, w) - \phi \hat{Z}(d, w)]^2. \quad (\text{B5})$$

We wish to calculate a 95% confidence interval for the difference between the frequency of minimum duration for the high and low phases of the NAO under the null hypothesis that the low- and high-phase runs have the same duration distributions. We create 10 000 model time series  $X$  as described above. The duration of a high-phase (low-phase) NAO event is defined as the number of consecutive days when  $Z$  is above (below)  $+1$  ( $-1$ ). For each time series, we compute the frequency of events with durations equal to or exceeding  $n$  days for both low- and high-phase events (as explained in the text). The 95th percentile of the difference between the low- and high-phase curves gives the 95% confidence interval for the difference. These calculations show that a higher frequency of occurrence of long-lasting low-phase events exists than for the high-phase events for durations 2–27 days.

## REFERENCES

- Ambaum, M., B. Hoskins, and D. Stephenson, 2001: Arctic Oscillation or North Atlantic Oscillation? *J. Climate*, **14**, 3495–3507.
- Benedict, J. J., S. Lee, and S. B. Feldstein, 2004: Synoptic view of the North Atlantic Oscillation. *J. Atmos. Sci.*, **61**, 121–144.
- Box, G. E. P., G. M. Jenkins, and G. C. Reinsel, 2008: *Time Series Analysis: Forecasting and Control*. 4th ed. John Wiley & Sons, 746 pp.
- Branstator, G., 1992: The maintenance of low-frequency atmospheric anomalies. *J. Atmos. Sci.*, **49**, 1924–1945.
- Eichelberger, S. J., and D. L. Hartmann, 2007: Zonal jet structure and the leading mode of variability. *J. Climate*, **20**, 5149–5163, doi:10.1175/JCLI4279.1.
- Feldstein, S. B., 1998: The growth and decay of low-frequency anomalies in a GCM. *J. Atmos. Sci.*, **55**, 415–428.
- , 2000: The timescale, power spectra, and climate noise properties of teleconnection patterns. *J. Climate*, **13**, 4430–4440.
- , 2003: The dynamics of NAO teleconnection pattern growth and decay. *Quart. J. Roy. Meteor. Soc.*, **129**, 901–924.
- , and S. Lee, 1998: Is the atmospheric zonal index driven by an eddy feedback? *J. Atmos. Sci.*, **55**, 3077–3086.
- Frankze, C., S. Lee, and S. B. Feldstein, 2004: Is the North Atlantic Oscillation a breaking wave? *J. Atmos. Sci.*, **61**, 145–160.
- Gerber, E. P., and G. K. Vallis, 2007: Eddy–zonal flow interactions and the persistence of the zonal index. *J. Atmos. Sci.*, **64**, 3296–3311.
- Hamming, R. W., 1989: *Digital Filters*. Prentice Hall, 284 pp.
- Hartmann, D. L., 2007: The atmospheric general circulation and its variability. *J. Meteor. Soc. Japan*, **85B**, 123–143.
- , and F. Lo, 1998: Wave-driven zonal flow vacillation in the Southern Hemisphere. *J. Atmos. Sci.*, **55**, 1303–1315.

- Holopainen, E. O., and A. H. Oort, 1981: On the role of large-scale transient eddies in the maintenance of the vorticity and enstrophy of the time-mean atmospheric flow. *J. Atmos. Sci.*, **38**, 270–280.
- Holton, J. R., 2004: *An Introduction to Dynamic Meteorology*. 4th ed. Elsevier Academic, 535 pp.
- Hoskins, B. J., I. N. James, and G. H. White, 1983: The shape, propagation, and mean-flow interaction of large-scale weather systems. *J. Atmos. Sci.*, **40**, 1595–1612.
- Hurrell, J. W., Y. Kushnir, G. Ottersen, and M. Visbeck, 2003: An overview of the North Atlantic Oscillation. *The North Atlantic Oscillation: Climatic Significance and Environmental Impact, Geophys. Monogr.*, Vol. 134, Amer. Geophys. Union, 1–36.
- Jin, F.-F., L.-L. Pan, and M. Watanabe, 2006: Dynamics of synoptic eddy and low-frequency flow interaction. Part I: A linear closure. *J. Atmos. Sci.*, **63**, 1677–1694.
- Lau, N.-C., and M. J. Nath, 1991: Variability of the baroclinic and barotropic transient eddy forcing associated with monthly changes in the midlatitude storm tracks. *J. Atmos. Sci.*, **48**, 2589–2613.
- Lorenz, D. J., and D. L. Hartmann, 2001: Eddy–zonal flow feedback in the Southern Hemisphere. *J. Atmos. Sci.*, **58**, 3312–3327.
- , and —, 2003: Eddy–zonal flow feedback in the Northern Hemisphere winter. *J. Climate*, **16**, 1212–1227.
- Martius, O., C. Schwierz, and H. Davies, 2007: Breaking waves at the tropopause in the wintertime Northern Hemisphere: Climatological analyses of the orientation and the theoretical LC1/2 classification. *J. Atmos. Sci.*, **64**, 2576–2592.
- Nakamura, H., and J. M. Wallace, 1990: Observed changes in baroclinic wave activity during the life cycles of low-frequency circulation anomalies. *J. Atmos. Sci.*, **47**, 1100–1116.
- , and —, 1991: Skewness of low-frequency fluctuations in the tropospheric circulation during the Northern Hemisphere winter. *J. Atmos. Sci.*, **48**, 1441–1448.
- North, G. R., T. L. Bell, R. F. Cahalan, and F. J. Moeng, 1982: Sampling errors in the estimation of empirical orthogonal functions. *Mon. Wea. Rev.*, **110**, 699–706.
- Rennert, K. J., and J. M. Wallace, 2009: Cross-frequency coupling, skewness, and blocking in the Northern Hemisphere winter circulation. *J. Climate*, **22**, 5650–5666.
- Robinson, W. A., 1991: The dynamics of low-frequency variability in a simple model of the global atmosphere. *J. Atmos. Sci.*, **48**, 429–441.
- , 1996: Does eddy feedback sustain variability in the zonal index? *J. Atmos. Sci.*, **53**, 3556–3569.
- , 2000: A baroclinic mechanism for the eddy feedback on the zonal index. *J. Atmos. Sci.*, **57**, 415–422.
- , 2006: On the self-maintenance of midlatitude jets. *J. Atmos. Sci.*, **63**, 2109–2122.
- Thompson, D. W., and J. M. Wallace, 1998: The Arctic Oscillation signature in the wintertime geopotential height and temperature fields. *Geophys. Res. Lett.*, **25**, 1297–1300.
- , and —, 2000: Annular modes in the extratropical circulation. Part I: Month-to-month variability. *J. Climate*, **13**, 1000–1016.
- Uppala, S. M., and Coauthors, 2005: The ERA-40 reanalysis. *Quart. J. Roy. Meteor. Soc.*, **131**, 2961–3012.
- Vallis, G. K., and E. P. Gerber, 2008: Local and hemispheric dynamics of the North Atlantic Oscillation. *Dyn. Atmos. Oceans*, **44**, 184–212.
- Walker, G. T., 1924: Correlation in seasonal variation of weather. IX. A further study of world weather. *Mem. Ind. Meteor. Dept.*, **24**, 275–333.
- Woollings, T., B. Hoskins, M. Blackburn, and P. Berrisford, 2008: A new Rossby wave–breaking interpretation of the North Atlantic Oscillation. *J. Atmos. Sci.*, **65**, 609–626.
- , A. Hannachi, B. Hoskins, and A. G. Turner, 2010: A regime view of the North Atlantic Oscillation and its response to anthropogenic forcing. *J. Climate*, in press.